# Cooperative H-Bonds of Macromolecules. 1. Binding of Low-Molecular-Weight Ligands to Polymers

**Jaroslav Kříž* and Jiří Dybal**

*Institute of Macromolecular Chemistry, Academy of Sciences of the Czech Republic, Heyrovsky Sq. 2, 162 06 Prague 6, Czech Republic*

*Received: March 16, 2005; In Final Form: May 11, 2005*

Equilibrium bindings of two low-molecular-weight hydrogen bond acceptor ligands, tetrahydrofuran (THF) and pyridine (PH), and their fully deuterated analogues (TDF, PD) with poly(4-vinylphenol) (PVF) and its low-molecular-weight model, a hydrogen bond donor 4-isopropylphenol (IPP), were studied using spectroscopic (NMR) and theoretical (ab initio SCF-DFT B3LYP/6-31G(d)) methods as a first step of a general study of cooperative hydrogen bonding of H-bond-donating and -accepting macromolecules. Two reliable experimental methods of measuring the fraction of H-bonded or free ligands, which can be used as an indirect tool in further studies of macromolecular cooperative binding, were devised and examined in this study. The methods are complementary and independent. They are based on one hand on $^2$H quadrupolar or $^1$H longitudinal NMR relaxation and, on the other hand, on $^2$H or $^1$H PFG NMR self-diffusion measurement, using the pulsed-field-gradient spin−echo (PGSE) and pulsed-field-gradient stimulated echo (PGSTE) methods. It was shown that both the relaxation and PFG methods need viscosity correction using as an internal standard a relatively inert compound of a relaxation/diffusion rate similar to that of the internal standard ($CDCl_3$ or HMDSO in the present case). After such normalization, the reliability of both methods was checked by calculating the equilibrium constants $K$ of binding under a variety of ligand/donor ratios $\beta$. Excepting the rather impractical region of low $\beta$ values, where cooperative self-association of the H-donating polymer takes place, both methods were found to be reasonably reliable. A slight anomaly in the relaxation behavior of pyridine and its stronger-than-expected binding to PVF was plausibly explained (using high-precision quantum mechanical calculations) by additional formation of weak C−H···O bonds to the neighboring units.

## Introduction

Cooperative behavior of weak electrostatic, H-bond or hydrophobic interactions has been recognized as crucial for the formation of natural or synthetic macromolecular complexes,[1−4] in particular those that are endowed with some specific function. Although hundreds or more individual examples of such cooperative binding were detected and studied, little systematic work has been done in this field except the study of cooperative electrostatic interactions[5−11] between oppositely charged macromolecules. The next logical step is to examine the cooperativity of other types of binding interactions, in particular hydrogen bond interactions. A quantitative study of this effect meets some difficulties, however. Although the hydrogen bond has been widely studied for half a century and ingenious methods of its detection and characterization were found,[12,13] it is far from simple to quantify a fraction of specific hydrogen binding in a liquid system. Take as an example a polymeric hydrogen-bond donor such as poly(4-vinylphenol) (PVF), whose cooperative interactions with a polymeric acceptor such as poly(4-vinylpyridine) (PVP) should be studied. PVF (like any other analogous polymer) in the bulk binds via multiple hydrogen bonds to other molecules of itself so that it can be dissolved only in a solvent that breaks these bonds by creating its own ones, i.e., a hydrogen-bond acceptor (a Lewis base) such as tetrahydrofuran (THF), dimethyl sulfoxide (DMSO), or pyridine (there are other prerequisites of being a good solvent, but this one is a sine qua non). In a solution of PVF, we thus already have most of its OH groups bound to the solvent by a H-bond very similar to that we are expecting to be formed between PVF and PVP. The usual tools of H-bond detection such as the OH or CH−(OH) chemical shift in NMR or frequency and intensity of the corresponding vibrations in infrared spectroscopy[12,13] are of little use in our case except the possible demonstration that the bond to PVP is somewhat stronger. The problem is even more pronounced in the case of the following experiment. The cooperative binding of PVP to PVF can be elegantly demonstrated by substituting monomer pyridine already bound to PVF for the very analogous pyridine groups of PVP. However, such substitution has almost no effect on basic NMR or IR spectra of either PVF or PVP. Thus the extent of PVP (or analogous) binding must be measured indirectly. One and probably the only possibility is to measure the extent of originally bound low-molecular-weight ligands liberated in the process.

In this study, we examine hydrogen bonding of two low-molecular-weight ligands (THF and pyridine) to a polymeric hydrogen-bond donor (PVF). In the course of this study, we develop and critically examine two complementary methods of measuring the extent of their binding, namely, NMR relaxation and pulsed-field-gradient self-diffusion measurements, and consider their subsequent use in indirect assessment of the degree of hydrogen binding of two complementary macromolecules.

* To whom correspondence should be addressed. E-mail: kriz@imc.cas.cz. Phone: +420-296809382. Fax: +420-296809410.

10.1021/jp051373v CCC: $30.25 
Published on Web 06/28/2005

## Experimental Section

**Materials Used and Sample Preparation.** Poly(4-vinylphenol) (PVF) ($M_w = 1.5 \times 10^4$ g/mol) and polystyrene ($M_w = 1.2 \times 10^5$ g/mol) were products of Polyscience, and 4-isopropylphenol (IPP) was a product of Aldrich; all chemicals were used as obtained. Tetrahydrofuran-$d_8$ (THD), pyridine-$d_5$ (PD), and chloroform-$d$ ($CDCl_3$) were products of Eurorad. Tetrahydrofuran (THF), pyridine (PH), and hexamethyldisiloxane (HMDSO) were products of Aldrich. All these substances were dried with molecular sieves before use. The measured solutions were transferred into a NMR tube, degassed under argon, and sealed.

**NMR Relaxation and PFG Measurements.** All NMR measurements were done with an upgraded Bruker Avance DPX 300 spectrometer ($^1$H frequency at 300.13 MHz) equipped with a Bruker PFG unit BGU2 and inverse-detection water-cooled PFG probe with a gradient range up to 1500 G/cm. $^2$H longitudinal relaxation measurements[14−16] were done at 46.071 MHz with a broadband probe using an inverse-recovery pulse sequence $d_1$-$\pi_x$-d$_2$-$\pi/2_{x,-x}$-FID, with $d_1 = 8$ s and $d_2$ incremented in 16 steps from 0.1 to 1.6 s. A total of 2048 points were collected in each of the 48 scans. The measurements were done without lock, usually at night to minimize outer magnetic influences. Each measurement was repeated at least five times, and the arithmetic mean of the resulting $T_1$ values (scattered less than ±3% rel) was taken. PFG diffusion experiments of the deutero compounds were measured at the $^2$H resonance, using the decoupler channel of a *z*-gradient inverse-detection probe. The pulse sequences were both those of pulsed gradient spin−echo (PGSE),[17] i.e., $d_1$-$\pi/2_x$-gr-$d_2$-$\pi_y$-$d_2$-gr-FID, and pulsed gradient stimulated echo (PGSTE),[18] i.e., $d_1$-$\pi/2_x$-gr-$\pi/2_x$-$d_2$-$d_2$-$\pi/2_x$-gr-FID, with $d_1 = 8$ s and $d_2 = 0.2$ s. The gradient of a 2 ms pulse was incremented from 10 to 50 G/cm in 16 steps. A total of 2048 points were collected in each of the 64 scans. Again, the measurements were done without lock and repeated at least five times (scatter ± 3% rel). Diffusion experiments with the polymer[10,19] PVF were done on $^1$H resonance with a deuterium lock using PGSTE sequence on a special water-cooled inverse-detection *z*-gradient probe, $d_2 = 0.02$ s, and the 1 ms gradient pulse incremented from 5 to 500 G/cm in 16 steps. The measurements were repeated three times with the scatter < 3%. The $^1$H NMR $T_{1\rho}$ experiments were done with an inverse-detection probe (inner channel) using a pulsed spin-lock (5 $\mu$s pulse with 15 $\mu$s delay) placed on the measured signal. Seven experiments were done with the spin-lock length incremented in the interval 0.01−0.70 s, the electromagnetic field $\omega_1$ being gradually stepped up from 4.6 to 17.4 $\times 10^3$ rad/s. $^1$H NMR $T_1$ experiments were done with the same probe using the inversion−recovery pulse sequence with 32 increments. At least five measurements were done for each $T_1$ value (scatter < 2% rel).

**Quantum Mechanical Calculations.** Ab initio molecular orbital calculations were performed using the GAUSSIAN 98 suite of programs.[20] Geometries have been fully optimized at the B3LYP level of density functional theory (DFT) with the 6-31G+(d) and 6-311G+(2d,p) basis sets and the second-order Møller−Plesset (MP2) level of theory with the 6-31G(d) basis set.

## Results and Discussion

As already indicated in the Introduction, the indirect method of measuring the degree of binding α of the pyridine groups in poly(4-vinylpyridine) (PVP) to poly(4-vinylphenol) (PVF) can be based on measuring the fraction of low-molecular-weight ligands (THF, pyridine) liberated from their binding to PVF by their substitution for PVP pyridine groups. For this, equilibrium binding of these ligands to PVF before and after adding PVP has to be established. In the following, two independent methods, namely, relaxation ($^2$H NMR quadrupolar and $^1$H NMR longitudinal) and PFG NMR self-diffusion rate measurement, are elaborated and the fraction of THF-$d_4$ (TDF) or pyridine-$d_5$ (PD) bound to PVF is examined by them. The equilibrium constants of binding at 300 K are established at a number of different concentrations of PVF. The detected anomalies are clarified using model measurements with 4-isopropylphenol (IPP) instead of PVF and high-level quantum mechanical calculations. Finally, the limitations of the use of the outlined methods are established.

**1. Utilizing Quadrupolar Relaxation for the Measuring of the Fraction of H-Bound Species under Fast Chemical Exchange.** In principle, $^1$H or $^{13}$C longitudinal or transverse dipolar relaxation could be used for this purpose. However, various possible complications by spin−spin coupling or cross-relaxation ($^1$H) or poor sensitivity ($^{13}$C) make the quadrupolar $^2$H relaxation a better choice. In the following, we shall assume that the longitudinal relaxation of deuterium nuclei proceeds exclusively by a quadrupolar mechanism. Although this is not exactly true for $^2$H, this assumption will not strongly influence our results. The quadrupolar relaxation of a spin $S = 1$ nucleus at one site has been shown[14,15] to proceed monoexponentially, according to the relation

$$I_z(t) = I_z(0)\exp(-R_1 t) \tag{1}$$

where $R_1$ is the relaxation rate

$$R_1 = \frac{3\pi^2}{2}(1+\eta^2/3)\left(\frac{e^2qQ}{h}\right)^2 \frac{\tau_c}{1+(\omega_0\tau_c)^2} \tag{2}$$

In eq 2, $(e^2qQ/h)$ is the quadrupolar coupling constant, $\eta$ is the asymmetry factor, and $\tau_c$ is the correlation time of the motion leading to relaxation. If the nucleus jumps between two various sites X and Y with the respective residence times $\tau_X$ and $\tau_Y$, the relaxation is described by modified Bloch (Solomon) equations[16] and is generally biexponential. However, if the rate of exchange between the sites is at least an order of magnitude larger than the relaxation rate, e.g., $(1/\tau_X) > > R_{1X}$, fast exchange can be considered to maintain the equilibrium at every moment of decay; that is, the total intensity obeys the equation

$$\frac{dI_z}{dt} = [-\varphi_X R_{1X} - (1-\varphi_X)R_{1Y}]I_z, \tag{3}$$

where $\varphi_X$ is the molar fraction of the site X in the system

$$\varphi_X = \frac{\tau_X}{(\tau_X+\tau_Y)} \tag{4}$$

(where $\tau_X$ is the mean residence time at the site X). Equation 3 leads to a monoexponential decay

$$I_z(t) = I_z(0)\exp\{-[\varphi_X R_{1X} + (1-\varphi_X)R_{1Y}]t\}. \tag{5}$$

In the case of hydrogen-bonded low-molecular-weight compounds, the conditions of eq 3 are fulfilled for deuterium relaxation ($R_{1X}$, $R_{1Y} \leq 10$, $\tau_X^{-1}$, $\tau_Y^{-1} \geq 10^6$ s$^{-1}$ due to low energy barrier of exchange).

One has to note on margin that eq 3 is a good approximation not only if the condition of fast exchange is fulfilled but, at the

same time, if the residence times at sites X and Y are at least an order of magnitude larger than the correlation time of the jump from X to Y or vice versa. Calculations based on height of the energy barrier place the latter near $10^{-11}$ s, whereas the geometrical mean of the residence time obtained from $T_{1\rho}$ experiments is in the range $10^{-6}-10^{-8}$ s so that the condition is fulfilled.

In practical research, the fulfillment of both conditions is checked by the strictly monoexponential decay in all measured relaxations.

If $R_1$, $R_{1F}$, and $R_{1B}$ are the respective relaxation rates in the actual system (experimentally measured value) and in the free (unbound) and bound state, the molar fraction of the bound state $\varphi$ thus can be obtained from the relation

$$\varphi = \frac{R_1 - R_{1F}}{R_{1B} - R_{1F}} \tag{6}$$

Equation 6 holds if $R_1$, $R_{1F}$, and $R_{1B}$ are measured under the same viscosity. The reason for this as well as the way of circumventing this condition can be understood from the following. Under conditions of extreme narrowing, which are usually met in fast exchanging systems involving low-molecular-weight compounds, eq 2 can be well approximated by

$$R_1 = \chi_Q \tau_c \tag{7}$$

The effective quadrupolar coupling constant $\chi_Q$ depends on the electric field gradient and its asymmetry at the nucleus. As these quantities do not differ appreciably in the H-bonded and free states, the difference between $R_{1B}$ and $R_{1F}$ is given almost exclusively by the difference between the respective correlation times of tumbling in the bound and free states, $\tau_{cB}$ and $\tau_{cF}$. Equation 7 holds for the extreme narrowing condition ($\omega_0\tau_c < 1$), which could not be well fulfilled for $R_{1B}$. At 46 MHz, the condition requires $\tau_c$ of the maximum order of $10^{-9}$ s, which can be met even for the bound state, considering the relatively free motion of the O−H···N bond (cf. below the fact that $R_{1B}$ is at most 50 times larger than $R_{1F}$).

For isotropic motion, we are allowed to approximate $\tau_c$ by the Debye formula

$$\tau_c = \frac{4\pi r^3 \eta}{3kT} \equiv \zeta(r,T)\eta \tag{8}$$

where $\eta$ is the effective viscosity of the medium and $r$ is the radius of a sphere motionally equivalent to the molecule. Thus $R_1$ should be linearly dependent on $\eta$. As $\eta$ usually is not known, this could present a serious problem in polymer systems with varied concentration and/or molecular weight of the polymers. Thus we have to eliminate the influence of $\eta$ by renormalizing the relaxation rates to some standard viscosity.

Having two mutually independent (not exchanging) species X and Y in the system, we should have (under extreme narrowing) a linear relation

$$R_{1X} = \frac{\chi_{QA}\zeta(r,T)_X}{\chi_{QB}\zeta(r,T)_Y} R_{1Y} \equiv \kappa_{AB} R_{1Y} \tag{9}$$

where $\kappa_{AB}$ is a constant at constant temperature.

Figure 1 shows a correlation of deuterium relaxation rates of TDF and $CDCl_3$ deuterons in differently concentrated (and thus differently viscous) solutions of polystyrene at 300 K. The linear relation assumed in eq 9 clearly holds. The slopes for α and $\beta$ deuterons in TDF are the same, as it can be expected considering that no specific interactions are present and the tumbling of TDF is very nearly isotropic.

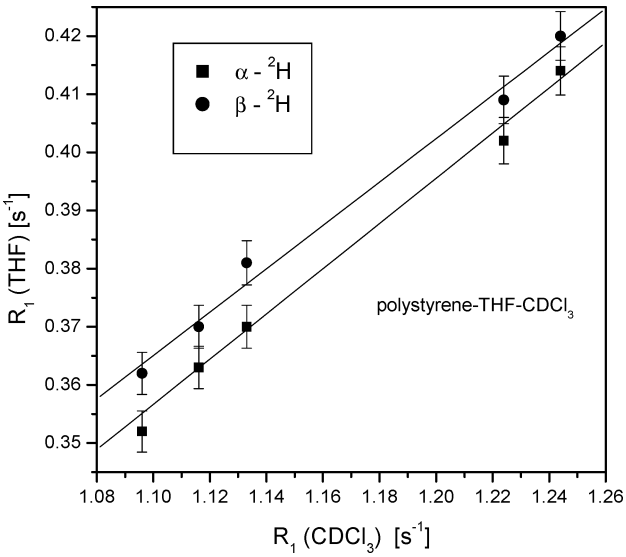


**Figure 1.** Correlation between $^2H$ longitudinal relaxation rates of TDF and $CDCl_3$ deuterons in differently concentrated solutions of polystyrene at 300 K.

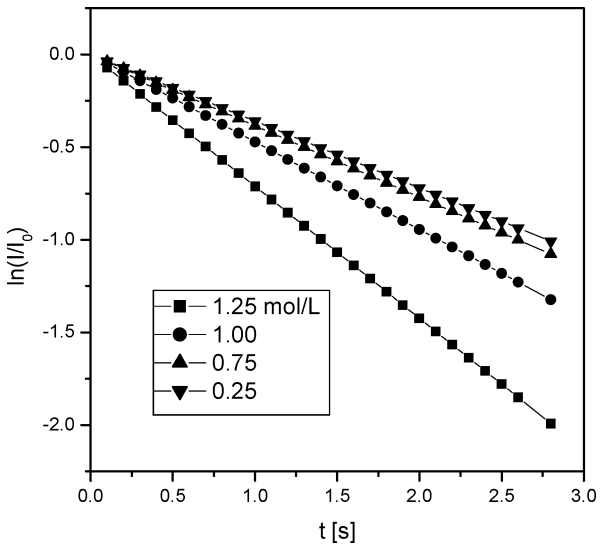


**Figure 2.** Logarithmic plots of the intensity of α deuterons of TDF in the presence of indicated amounts of PVF (in molar concentration of OH groups) at 300 K.

A different situation arises in systems containing poly-(4-vinylphenol) (PVF) instead of polystyrene. Here, the polymer increases the viscosity again but, additionally, binds a part of TDF (in contrast to $CDCl_3$) in a faster-relaxing H-bonded state. As it is shown in Figure 2 for TDF α deuterons, the relaxation decay is still strictly monoexponential.

The correlation between the obtained relaxation rates $R_1$ of TDF and added $CDCl_3$ is linear again, as shown in Figure 3, but the respective slopes for α and $\beta$ deuterons are markedly different: 0.99 and 0.57 (± 0.04) at 300 K and 0.64 and 0.43 (± 0.03) at 320 K. As there is no reason the quadrupolar coupling constant should significantly change with viscosity, which is the same for both TDF and $CDCl_3$ in the given system, the differences in slopes for α and $\beta$ deuterons must be due to interaction of TDF with PVF. Relaxation thus clearly reflects H-bond interaction of TDF with PVF (under reasonable assumption that the motion in the bound state is anisotropic, see below).

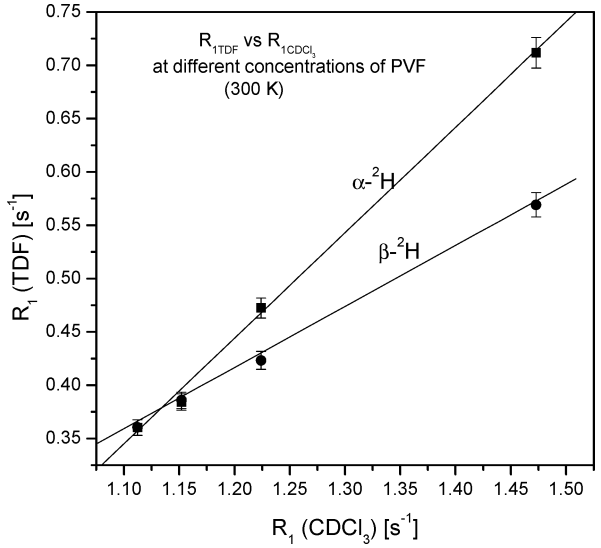


**Figure 3.** Correlation between $^2$H longitudinal relaxation rates of TDF and $CDCl_3$ deuterons in differently concentrated solutions of poly-(4-vinylphenol) at 300 K.

A similar picture can be obtained with PD substituting or mixed with TDF. In principle, quadrupolar relaxation thus can be utilized for measuring the equilibrium constants of TDF-PVF and PD-PVF. However, raw $R_1$, $R_{1F}$, and $R_{1B}$ have to be normalized to the same viscosity. This can be done utilizing eq 9 in the following way. Adding to each of the examined systems (one of which is considered to be the standard system S) a certain amount of a deuterated compound C, which does not chemically interact with any of its component, we can calculate the viscosity-normalized value $R_1^N$ from the simple relation

$$R_1^N = R_1 R_{1C}^S / R_{1C} \tag{10}$$

where $R_{1C}$ and $R_{1C}^S$ are the relaxation rates of C measured in the given and the standard system, respectively. An analogy of eq 6, namely,

$$\varphi = \frac{R_1^N - R_{1F}^N}{R_{1B}^N - R_{1F}^N} \tag{11}$$

(where $R_{1F}^N$ and $R_{1B}^N$ are obtained in an analogous way as $R_1^N$) then holds irrespective of the viscosity of the system.

$R_{1F}$ can be obtained simply in the solution of the ligand (or in a neat compound in a case such as TDF), but $R_{1B}$ cannot be measured directly. Assuming that $R_{1B}$ does not depend on the number of ligand molecules bound to the polymer (i.e., there is a single value of $R_{1B}$ for all ligand-to-polymer ratios), its value can be obtained by extrapolation of $R_1^N$ to some extreme value of $\beta$. The one possibility, $\beta \rightarrow 0$, is hampered by the fact that systems with $\beta < 3$ cannot be easily prepared and measured. In addition, self-association of the polymer (PVF) takes place in highly concentrated solutions, which interferes with the measured binding as shown below. Therefore, the other extreme, $\beta \rightarrow \infty$, must be used in the following way. Let $\varphi_{max}$ be the maximal attainable molar fraction of the bound ligand at the given $\beta$ (i.e., the fraction corresponding to the situation when all sites of the polymer are occupied by the ligand). Clearly, $\varphi_{max} = 1/(\beta - 1)$. The actual value of $\varphi$ is lower than $\varphi_{max}$ at any finite $\beta$ but converges to it at $\beta \rightarrow \infty$. Assuming $\varphi = \varphi_{max}$,

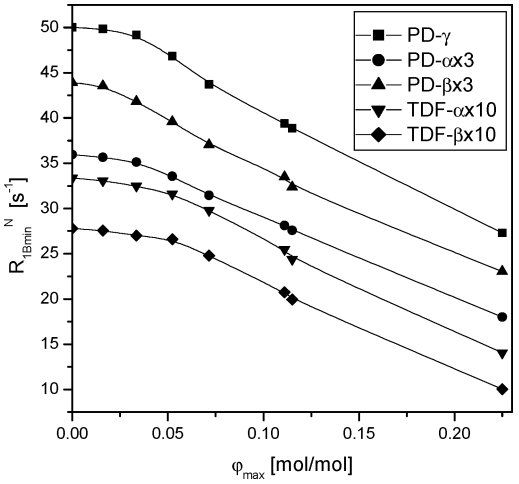


**Figure 4.** Calculated $^2$H $R_{1Bmin}^N$ relaxation rates of indicated deuterons of PD and TDF at different ratios $\beta$ = [base]/[OH] in PD or TDF solutions of PVF at 300 K.

we get the minimal value of $R_{1B}^N$ at the given $\beta$, $R_{1Bmin}^N$:

$$R_{1Bmin}^N = \frac{R_1^N - R_{1F}^N(1 - \varphi_{max})}{\varphi_{max}} \tag{12}$$

This value converges to the true $R_{1B}^N$ as $\varphi$ converges to $\varphi_{max}$, i.e., at $\beta \rightarrow \infty$ ($\varphi_{max} \rightarrow 0$).

The measured dependences of $R_{1Bmin}^N$ on $\varphi_{max}$ are shown in Figure 4 for deuterons of PD and TDF in the respective solutions of PVF. All dependences converge fairly well. Thus the extrapolated values of $R_{1Bmin}^N$ (the points at $\varphi_{max} = 0$) should be identified with the corresponding values of $R_{1B}^N$.

Such a procedure is based on the assumption that the value of $R_{1B}^N$ is independent of the number of ligand molecules bound to PVF molecule. As shown below, this is approximately true for TDF but not for PD.

**2. Utilizing $^1$H NMR Longitudinal Relaxation for the Establishment of the Fraction of H-Bound Species under Fast Chemical Exchange.** Although $^2$H quadrupolar relaxation is generally preferable for the present needs, there is no serious objection against the use of $^1$H longitudinal relaxation for the same ends providing that conditions of fast exchange and extreme narrowing are met: in contrast to transverse relaxation, the longitudinal one depends mostly on the rotational mobility of the respective sites and is not influenced by the process of chemical exchange. $^1$H longitudinal relaxation is used below in the check of absence of an isotopic effect in PD binding to a H-bond donor.

If two species X and Y bind together, forming an adduct XY in an equilibrium, the respective longitudinal relaxation rates of chosen protons in them are

$$R_{1X} = (1 - \varphi)R_{XF} + \varphi R_{XB} \tag{13}$$

$$R_{1Y} = (1 - \beta\varphi)R_{YF} + \beta\varphi R_{YB} \tag{14}$$

where $R_{1X}$, $R_{XF}$, and $R_{XB}$ are the relaxation rates of X actually measured at $\beta = [X]_0/[Y]_0$, in the purely unbound (free) and purely bound state, respectively. Again, all relaxation rates must be viscosity-normalized. In eqs 13 and 14, $R_{1X}$, $R_{1Y}$, $R_{XF}$, and $R_{YF}$ can be independently measured and $\beta$ is given so that we have three unknown quantities: $\varphi$, $R_{XB}$, and $R_{YB}$. Evidently, one experiment is not enough for establishing them, but two experiments with different values of $\beta$, say $\beta_1$ and $\beta_2$, offer four

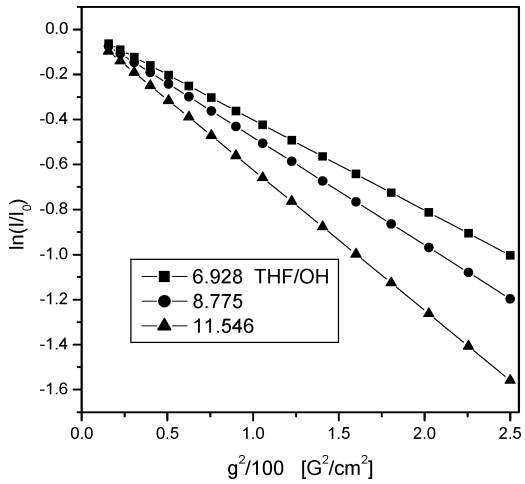


**Figure 5.** Logarithmic dependences of relative signal intensity of TDF $^2$H NMR signals on the square of field gradient in PGSE of PVF-TDF systems with the indicated THF/OH molar ratios at 300 K.

equations with four unknowns: $\varphi_1$, $\varphi_2$, $R_{XB}$, and $R_{YB}$. Two experiments thus are sufficient, but considering the unavoidable errors of measuring relaxation rates and their normalization to the same viscosity, a higher number of experiments with a subsequent optimization of parameters is preferable. This method is particularly suitable for the examination of binding between two proton-bearing low-molecular-weight compounds as shown below.

**3. Utilizing PFG Self-Diffusion Measurement for the Establishment of the Fraction of H-Bound Species under Fast Chemical Exchange.** The use of a PFG self-diffusion measurement under fast exchange of the free and bound species follows the same logic as above because the dephasing of nuclear spins by the field gradient is a process in many respects analogous to relaxation.[17,18] If the exchange is more than 1 order of magnitude faster than diffusion, the signal attenuation by progressively growing pulsed-field-gradient $g$ obeys a monoexponential relation[17]

$$I(g) = I(0)\exp[-\gamma^2 g^2 \delta^2 D(\Delta - \delta/3)] \qquad (15)$$

where $\gamma$ is the gyromagnetic ratio for the given nucleus ($^1$H in our case), $\delta$ the pulse length, and $\Delta$ diffusion delay (held constant in our experiments). Under fast exchange, the effective diffusion coefficient $D$ can be expressed as

$$D = (1 - \varphi)D_F + \varphi D_B \qquad (16)$$

where $\varphi$ is again the molar fraction of the bound species and $D_F$ and $D_B$ are diffusion coefficients of the free and bound species. The validity of the monoexponential relation (eq 15) in our case is demonstrated for the system PVF-THF in Figure 5, where logarithmic dependences of signal intensity on $g^2$ are given for various THF/OH molar ratios.

In analogy with eq 9, we thus could obtain the fraction of the bound THF from the relation

$$\varphi = \frac{D_F - D}{D_F - D_B} \qquad (17)$$

where $D_F$ and $D_B$ are the translation self-diffusion coefficients of the free and bound species, respectively. In analogy with relaxation, however, all the diffusion coefficients in eq 17 depend on viscosity as expressed in the Stokes−Einstein relation

$$D = kT/8\pi R_H \eta \equiv \xi(R_H,T)/\eta \qquad (18)$$

where $R_H$ is the hydrodynamic radius.

In systems with different viscosities, we thus should obtain a linear correlation between diffusion coefficients of two independent species in analogous systems with different viscosities. This is really so for the diffusion coefficients of TDF and $CDCl_3$ in variously concentrated solutions of polystyrene and PVF, where the slopes are $(1.044 \pm 0.5) \times 10^{-3}$ and $(1.083 \pm 0.5) \times 10^{-3}$, respectively. The higher value in the latter case is certainly due to slight binding of TDF by PVF.

In close analogy with eqs 10 and 11, we thus can define a viscosity-normalized diffusion coefficient $D^N$:

$$D^N = DD_C^S/D_C \qquad (19)$$

where $D_C$ and $D_C^S$ are the diffusion coefficients of some noninteracting species C in the given and a standard system, respectively. Again, the generally valid form of eq 17 is

$$\varphi = \frac{D_F^N - D^N}{D_F^N - D_B^N} \qquad (20)$$

Generally, the value of $D_B$ (and $D_B^N$) is not known. If the binding site is a polymer, $D_B$ should be equal to its diffusion coefficient in the actual system, $D_P$. In special cases, some chains could be actually poor in ligand occupancy or entirely free of it. Under fast exchange, however, all chains are statistically allotted the same fraction of the ligand during the diffusion period so that, from this point of view, they exhibit the same diffusion behavior.

In some cases, larger polydispersity of molecular weights could lead to a log-normal distribution of self-diffusion coefficients.[10,19] In practice, the PGSTE decays can be fitted by a polyexponential (usually biexponential) function:

$$I(g) = I(0)\sum_{i=1}^{n} w_i \exp[D_{Pi}\gamma_i^2 \delta^2 g^2(\Delta - \delta/3)] \qquad (21)$$

where $w_i$ is the corresponding statistical weight. Although eq 21 does not describe the behavior of the system exactly, it is empirically a good approximation. To get a single value of $D_B$, we have to add another approximation based on the following reasoning. As already said above, the monoexponential shape of PGSE decay of PD (and other low-molecular-weight ligands') signals shows that the exchange between bound and free states is much faster than diffusion along the axis of the field gradient. In other words, a great number of exchange jumps is accomplished during the diffusion delay $\Delta$. Thus the probability that a "tagged" PD molecule is bound (and unbound) to different polymer molecules during that period is large. In such a case, we are allowed to use the approximation

$$D_B = \sum_{i=1}^{n} w_i D_{Pi} \qquad (22)$$

where both $w_i$ and $D_{Pi}$ are obtained from the fitting using eq 21. Using eq 19, we obtain $D_B^N$. This approach was needed in the present case of PVF.

There is an alternative approach suitable especially for binding of two low-molecular-weight compounds, which entirely avoids measuring $D_B$. Let us assume again two species X and Y, the

**TABLE 1: $^2$H Longitudinal Relaxation Rates $R_1$ and $R_1^N$ and Self-Diffusion Coefficients $D$ and $D^N$ of TDF in Its Mixtures with PVF and the Corresponding Fractions of Bound TDF $\varphi$ and Equilibrium Constants $K$ at 300 K[a]**

| | $^2$H relaxation | | | | PFG diffusion | | | |
|---|---|---|---|---|---|---|---|---|
| $\beta$ mol/mol | $R_1$ $s^{-1}$ | $R_1^N$ $s^{-1}$ | $\varphi$ mol/mol | $K$ L/mol | $D$ $m^2/s\times10^9$ | $D^N$ $m^2/s\times10^9$ | $\varphi$ mol/mol | $K$ L/mol |
| 6.293 | 0.811 | 0.757 | 0.132 | 0.70 | 2.403 | 2.460 | 0.130 | 0.63 |
| 8.775 | 0.693 | 0.664 | 0.101 | 1.08 | 2.592 | 2.615 | 0.100 | 1.00 |
| 11.546 | 0.603 | 0.599 | 0.079 | 1.47 | 2.713 | 2.726 | 0.079 | 1.42 |
| 25.921 | 0.471 | 0.469 | 0.036 | 1.53 | 2.899 | 2.955 | 0.036 | 1.50 |
| 50.211 | 0.420 | 0.418 | 0.018 | 1.53 | 2.999 | 3.046 | 0.018 | 1.51 |

[a] $R_{1F}^N = 0.363\ s^{-1}$, $R_{1B}^N = 3.336\ s^{-1}$, $D_F^N = 3.142 \times 10^{-9}\ m^2/s$, $D_B^N = (1.123-2.103) \times 10^{-10}\ m^2/s$.

first being the binding ligand and the second a binding site (not necessarily on a polymer). Again, we have $[X]_0/[Y]_0 = \beta$, $([X]_0 - [X])/[X]_0 = \varphi$, $([Y]_0 - [Y])/[Y]_0 = \beta\varphi$. Under the condition of fast exchange, the following relations hold:

$$D_X = (1 - \varphi)D_{XF} + \varphi D_B \tag{23a}$$

$$D_Y = (1 - \beta\varphi)D_{YF} + \beta\varphi D_B \tag{23b}$$

where $D_X$ and $D_Y$ are the actually measured coefficients of species X and Y, respectively, and $D_{XF}$ and $D_{YF}$ are their values in the free (unbound) state. $D_B$ is the coefficient of the actually bound species, which is the same for both X and Y. By elementary algebraic manipulation, we get

$$\varphi = \frac{\beta(D_{XF} - D_X) - (D_{YF} - D_Y)}{\beta(D_{XF} - D_{YF})} \tag{24}$$

In eq 24, all variables can be measured independently and no assumption about $D_B$ is needed. The practical use of this equation requires, of course, correction of all coefficients to the same viscosity as explained above.

**4. Establishment of Equilibrium Constants of Binding of TDF and PD to PVF Using Quadrupolar Relaxation and PFG Diffusion Measurements.** For one partially bound species A, the equilibrium constant $K$ of binding to binding sites B can be obtained from the relation

$$K = \frac{\varphi[A]_0}{(1 - \varphi)[A]_0([B]_0 - \varphi[A]_0)} = \frac{\varphi}{(1 - \varphi)[(1/\beta) - \varphi]}\frac{1}{[A]_0} \tag{25}$$

where $\varphi$ is the molar fraction of the bound species A and $\beta$ is the molar ratio of the species A under study to the binding sites (e.g., PD or TDF to OH of PVF in our case) and $[A]_0$ is its initial concentration in mol/L. Tables 1 and 2 show results for TDF-PVF and PD-PVF systems at 300 K.

For a better overview of the results, the apparent values of $K$ are plotted against $\beta$ in Figures 6 and 7 for TDF and PD, respectively. The calculated $K$ is evidently not constant in the whole range of $\beta$ for either of the ligands. In addition, for PD there is a difference between the results derived from relaxation and those from PFG self-diffusion measurements. The common feature of all plots is the approximately 2-fold increase of the apparent $K$ in the interval of $\beta$ between 0 and 10. This behavior can be understood by comparing Figures 6 and 7 with the plots in Figure 8, where the normalized self-diffusion coefficients of PVF undergo a similar increase in the same interval. The only reason the normalized (i.e., viscosity-corrected) diffusion coefficient should decrease at lower $\beta$ (i.e., higher polymer concentration) is the self-association of PVF due to intermolecular hydrogen bonds. This type of binding clearly competes with that of PVF with the solvent ligands, leading thus to the observed decrease of the apparent value of $K$. Fortunately, the interval of $\beta$, in which such competition effectively interferes, is rather impractical for the study of cooperative binding of polymers so that it does not prevent the use of methods outlined here.

The difference between relaxation and diffusion results in the case of pyridine at $\beta > 10$ is a more intriguing feature. Although the value of $K$ is extremely sensitive to small errors of $\varphi$ (at the fourth decimal place, not shown in Table 2) at large

**TABLE 2: $^2$H Longitudinal Relaxation Rates $R_1$ and $R_1^N$ and Self-Diffusion Coefficients $D$ and $D^N$ of PD in Its Mixtures with PVF and the Corresponding Fractions of Bound PD $\varphi$ and Equilibrium Constants $K$ (same dimensions as in Table 1) at 300 K[a]**

| | | $\beta$ | | | | | | |
|---|---|---|---|---|---|---|---|---|
| | | 5.444 | 9.678 | 9.980 | 14.971 | 20.130 | 30.849 | 63.361 |
| $\alpha$-$^2$H | $R_1$ | 3.113 | 2.221 | 2.190 | 1.799 | 1.583 | 1.393 | 1.209 |
| | $R_1^N$ | 2.918 | 2.120 | 2.088 | 1.736 | 1.554 | 1.369 | 1.191 |
| | $\varphi$ | 0.173 | 0.100 | 0.097 | 0.065 | 0.049 | 0.032 | 0.016 |
| | $K$ | 1.99 | 3.74 | 3.86 | 4.46 | 4.86 | 5.18 | 5.44 |
| $\beta$-$^2$H | $R_1$ | 3.832 | 2.675 | 2.632 | 2.098 | 1.823 | 1.583 | 1.311 |
| | $R_1^N$ | 3.611 | 2.545 | 2.502 | 2.031 | 1.788 | 1.541 | 1.303 |
| | $\varphi$ | 0.173 | 0.100 | 0.097 | 0.065 | 0.049 | 0.032 | 0.016 |
| | $K$ | 2.01 | 3.76 | 3.90 | 4.48 | 4.88 | 5.21 | 5.40 |
| $\gamma$-$^2$H | $R_1$ | 9.943 | 6.534 | 6.013 | 4.394 | 3.568 | 2.723 | 1.876 |
| | $R_1^N$ | 9.754 | 6.403 | 5.962 | 4.355 | 3.524 | 2.681 | 1.867 |
| | $\varphi$ | 0.173 | 0.100 | 0.097 | 0.065 | 0.049 | 0.032 | 0.016 |
| | $K$ | 2.02 | 3.78 | 3.88 | 4.52 | 4.92 | 5.22 | 5.46 |
| PFG | $D \times 10^9$ | 1.235 | 1.399 | 1.584 | 1.643 | 1.689 | 1.718 | 1.761 |
| | $D^N \times 10^9$ | 1.453 | 1.598 | 1.604 | 1.669 | 1.703 | 1.736 | 1.769 |
| | $\varphi$ | 0.173 | 0.101 | 0.098 | 0.065 | 0.049 | 0.032 | 0.016 |
| | $K$ | 2.01 | 4.28 | 4.35 | 4.91 | 5.19 | 5.12 | 5.38 |

[a] $R_{1F}^N = 1.021$ ($\alpha$), 1.076 ($\beta$), and 1.092 ($\gamma$) $s^{-1}$, $R_{1B}^N = 11.98$ ($\alpha$), 14.64 ($\beta$), and 50.01 ($\gamma$) $s^{-1}$, $D_F^N = 1.800 \times 10^{-9}\ m^2/s$, $D_B^N = (1.282-2.019) \times 10^{-10}\ m^2/s$.

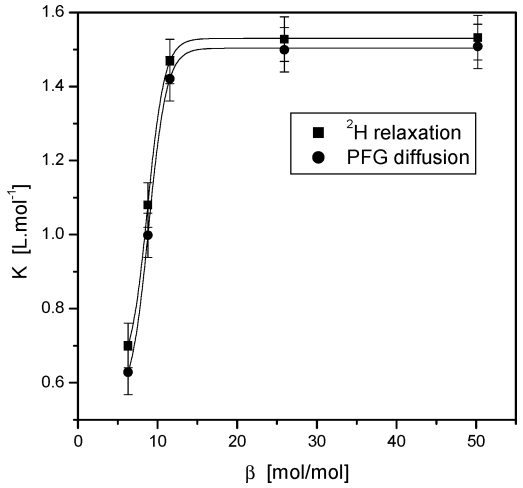


**Figure 6.** Apparent values of the equilibrium constant $K$ (calculated from relaxation and diffusion experiments) of TDF binding to PVF in dependence on $[TDF]_0/[OH]_0$ molar ratios at 300 K.

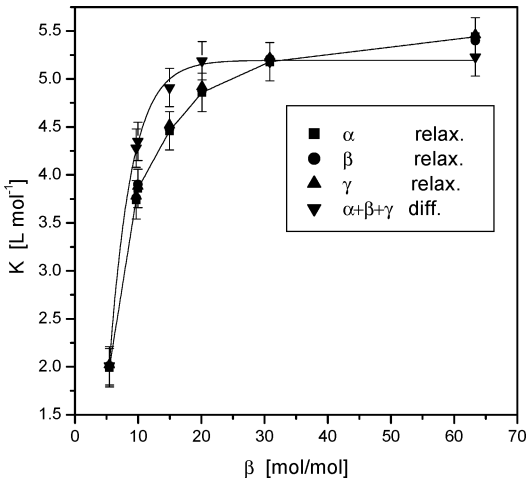


**Figure 7.** Apparent values of the equilibrium constant $K$ (calculated from relaxation and diffusion experiments) of PD binding to PVF in dependence on $\beta = [PD]_0/[OH]_0$ molar ratios at 300 K.

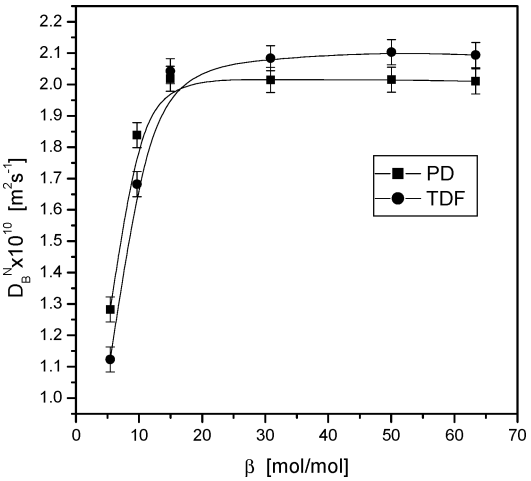


**Figure 8.** Weighted and normalized self-diffusion coefficients of PVF (PGSTE, $\delta = 1$ ms, $\Delta = 0.2$ s, $g = 5-500$ G/cm) in TDF and PD solutions at various $\beta$ ratios and 300 K.

$\beta$ values, there is a definite increase in $K$ derived from relaxation in the region where those from PFG measurements are already constant. Although the difference between the results from both methods almost does not exceed the limits of expected error, the behavior of relaxation is worth examination from a methodological point of view.

The only possible explanation of this phenomenon is that $R_{1B}^N$ is not constant in the whole range of $\beta$ as originally supposed. This observation will be discussed below.

**5. Binding of PD and PY to a Low-Molecular-Weight Model of PVF and Its Effect on Relaxation.** To clarify the somewhat anomalous behavior of PD relaxation bound to a polymer, we substituted PVF by its low-molecular-weight model, namely, 4-isopropylphenol (IPP). The relaxation method used was quite analogous to that described above. The results are given in Table 4. As it can be expected, there is a lower difference between the relaxation rates of α, $\beta$, and in particular $\gamma$ deuterons in the bound PD. The reason for this is the much higher contribution of the overall tumbling of the IPP-PD aggregate to the motion causing relaxation, which is approximately the same for all deuterons.

The relaxation data in Table 3 match those from PFG measurements quite well; no anomaly is observed except a slight decrease of apparent $K$ at low $\beta$ values. This decrease is caused

**TABLE 3: $^2$H Longitudinal Relaxation Rates $R_1$ and $R_1^N$ and Self-Diffusion Coefficients $D$ and $D^N$ of PD in Its Mixtures with IPP and the Corresponding Fractions of Bound PD $\varphi$ and Equilibrium Constants $K$ (same dimensions as in Table 1) at 300 K[a]**

| | | $\beta$ | | | |
|---|---|---|---|---|---|
| | | 3.31 | 9.87 | 22.54 | 61.95 |
| α-$^2$H | $R_1$ | 4.081 | 2.089 | 1.484 | 1.182 |
| | $R_1^N$ | 3.922 | 2.003 | 1.452 | 1.178 |
| | $\varphi$ | 0.290 | 0.098 | 0.043 | 0.016 |
| | $K$ | 3.53 | 3.63 | 3.60 | 3.61 |
| $\beta$-$^2$H | $R_1$ | 2.732 | 1.693 | 1.343 | 1.165 |
| | $R_1^N$ | 2.639 | 1.605 | 1.308 | 1.161 |
| | $\varphi$ | 0.290 | 0.098 | 0.043 | 0.016 |
| | $K$ | 3.54 | 3.61 | 3.61 | 3.63 |
| $\gamma$-$^2$H | $R_1$ | 2.158 | 1.494 | 1.274 | 1.148 |
| | $R_1^N$ | 2.039 | 1.413 | 1.233 | 1.143 |
| | $\varphi$ | 0.291 | 0.098 | 0.043 | 0.016 |
| | $K$ | 3.55 | 3.64 | 3.66 | 3.64 |
| PFG | $D \times 10^9$ | 2.048 | 3.146 | 3.403 | 3.602 |
| | $D^N \times 10^9$ | 2.127 | 3.164 | 3.462 | 3.610 |
| | $\varphi$ | 0.290 | 0.098 | 0.043 | 0.016 |
| | $K$ | 3.54 | 3.62 | 3.64 | 3.66 |

$R_{1F}^N = 1.021$ (α), 1.076 ($\beta$), and 1.092 ($\gamma$) s$^{-1}$, $R_{1B}^N = 11.009$ (α), 6.459 ($\beta$), and 4.354 ($\gamma$) s$^{-1}$, $D_F^N = 3.694 \times 10^{-9}$ m$^2$/s, $D_B^N = 1.7005 \times 10^{-9}$ m$^2$/s.

**TABLE 4: $^1$H Longitudinal Normalized Relaxation Rates $R_1^N$ of PH in Its Mixtures with IPP and the Corresponding Optimized Fractions of Bound PH $\varphi$ and Equilibrium Constants $K$ (same dimensions as in Table 1) at 300 K[a]**

| $[X]_0$ | $\beta$ | $R_{1X}^N$ | $R_{1Y}^N$ | $\varphi$ | $K$ |
|---|---|---|---|---|---|
| 0.2090 | 1.00 | 0.3271 | 0.2591 | 0.3371 | 3.67 |
| 0.3156 | 3.26 | 0.1451 | 0.2552 | 0.1528 | 3.71 |
| 0.0891 | 1.07 | 0.2782 | 0.2417 | 0.1937 | 3.64 |
| 0.0565 | 0.45 | 0.3319 | 0.1318 | 0.2859 | 3.66 |
| 0.3579 | 10.72 | 0.1078 | 0.2611 | 0.0526 | 3.82 |

[a] $R_{XF}^N = 0.0936$ (α), $R_{YF}^N = 0.1743$ (α) s$^{-1}$, optimized: $R_{XB}^N = 0.3949$ (α), $R_{YB}^N = 0.2664$ (α) s$^{-1}$.

again by the self-binding of IPP, which competes with PD binding much less than that of PVF under analogous conditions. Hence the H-bonding self-association of PVF has some degree of cooperativity.

To check the possible (if improbable) deuterium isotopic effect in PD binding and, at the same time, the use of longitudinal $^1$H relaxation for the determination of the binding degree (see paragraph 2), we examined the binding of PH (normal pyridine) to IPP. In this case, the system was a $CDCl_3$ solution of both reactants with added HMDSO as internal standard, the concentration of PH (named $[X]_0$ in accord with the above formulas) being in a much lower range of 0.05−0.4 mol/L. The results obtained from five experiments, namely, measured relaxation rates $R_{1X}^N$ and $R_{1Y}^N$, optimized values of $\varphi$, $R_{XB}$, and $R_{YB}$, and the calculated values of $K$ for each experiment, are given in Table 4 ($R_1$ values of α protons of both PH and IPP given here only). As it can be seen, the values are the same as for PD within reasonable experimental error. Hence, no marked isotopic effect is observed and PH behaves in a normal way, too.

The fact that no anomaly is observed in either the PD or PH relaxation in the respective systems shows that the gradual increase of $R_{1B}^N$ in PD binding to PVF must be due to the vicinity of neighboring OH groups in PVF. A plausible explanation of this effect is given in the next paragraph.

On margin, note the differences in deuterium relaxation time in PD free, bound to PVF, and bound to IPP. As shown in Scheme 1, these must be due to differences in the axis of the

**SCHEME 1**

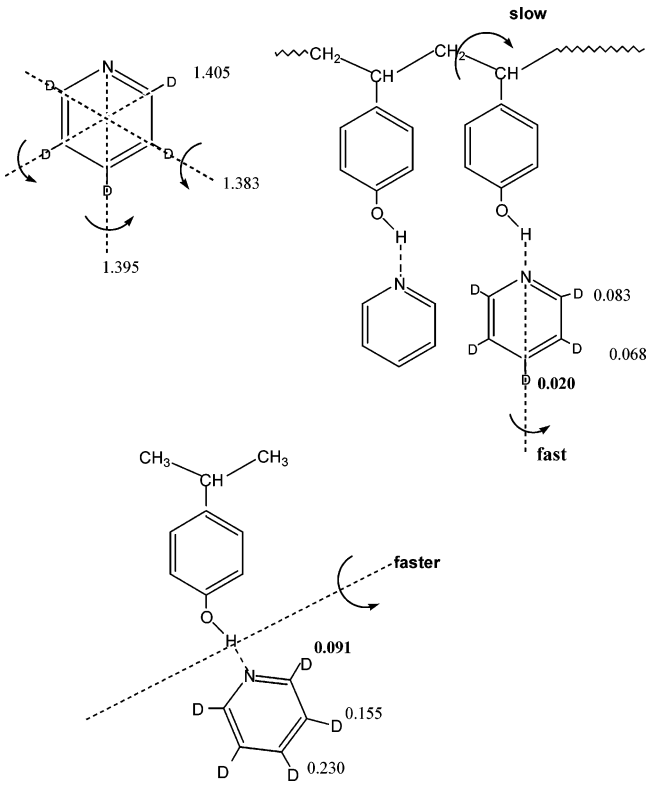


**TABLE 5: Total Energies *E* and Binding Energies Δ*E* (kcal/mol) for 4-Methylphenol (MePh), Pyridine (PH), Tetrahydrofuran (THF), Syndiotactic and Isotactic Hexa(4-vinylpenol) ($VF_6$), and the Corresponding H-Bonded Adducts in Structures Calculated and Fully Optimized by ab Initio SCF-DFT (B3LYP/6-31G(d)) Calculation**

| | *E* | Δ*E* |
|---|---|---|
| MePh | −346.7822486 | |
| PH | −248.2849729 | |
| THF | −232.4494431 | |
| MePh-PH | −595.0832415 | −10.05 |
| $PVF_6$-syn | −2349.864159 | |
| $PVF_6$-syn-$PH_6$ | −3839.685218 | −11.63 |
| $PVF_6$-iso | −2349.849976 | |
| $PVF_6$-iso-$PH_6$ | −3839.676454 | −12.20 |
| MePh-THF | −579.2476381 | −10.01 |
| $PVF_6$-syn | −2349.864159 | |
| $PVF_6$-syn-THF | −3744.663731 | −10.76 |
| $PVF_6$-iso | −2349.849976 | |
| $PVF_6$-iso-THF | −3744.649264 | −10.73 |

main rotational diffusion causing the relaxation: the free PD molecule tumbles in an isotropic way; PD bound to a polymer rotates mainly around the axis in the direction of the N−H bond so that the $\gamma$ deuteron exhibits the fastest relaxation; in a PD-IPP adduct, this rotation is surely important, but a rotation around an axis bisecting the adduct must be more important as $\alpha$ deuterons have the lowest relaxation time in this case.

**6. Quantum Mechanical Calculations of the Binding of Pyridine or THF to PVF.** The present reliability of high-precision quantum mechanical calculations gives us the possibility to derive meaningful predictions about bonding from them. The penalty of it is the need to restrict our considerations to relatively small systems in vacuo. Nonetheless, the following results give interesting insight into our problems. Table 5 compares the predicted binding energies of pyridine (PH) or tetrahydrofuran (THF) with a monomeric model 4-methylphenol (MePh) to those with PVF. In our experiments, PVF is atactic with probably some prevalence of syndiotactic triads. In calculation, we have to examine both syndiotactic and isotactic polymers.

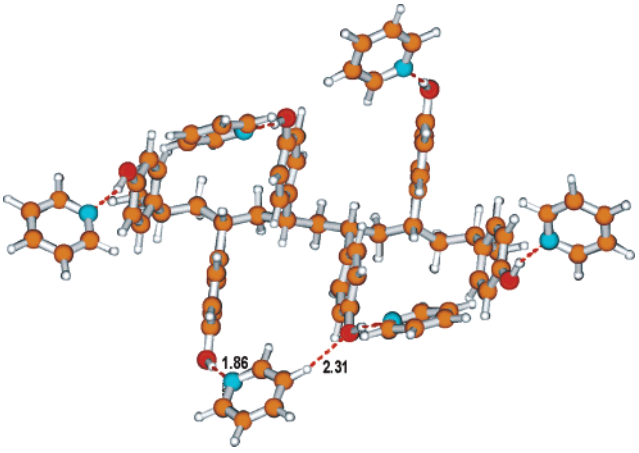


**Figure 9.** Fully optimized structure of the H-bonded adduct of pyridine with syndio-hexa(4-vinylphenol) (B3LYP/6-31G(d)).

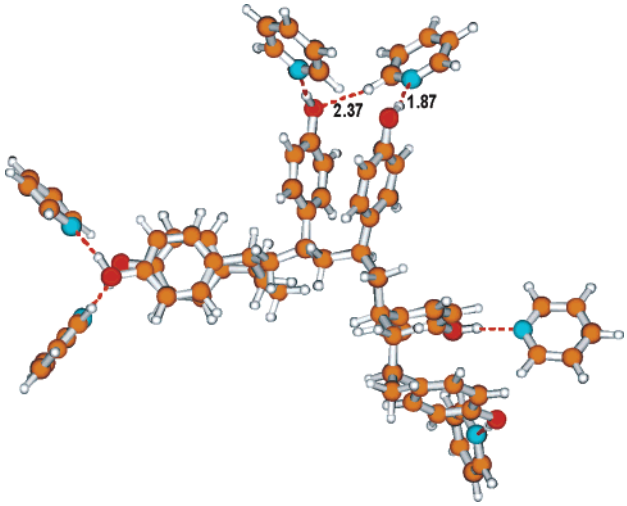


**Figure 10.** Fully optimized structure of the H-bonded adduct of pyridine with iso-hexa(4-vinylphenol) (B3LYP/6-31G(d)).

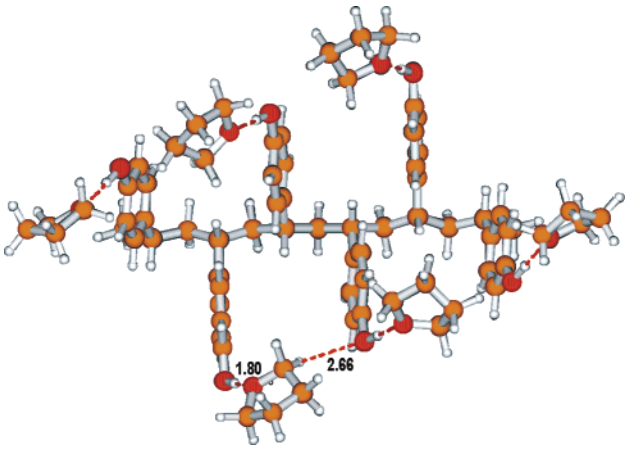


**Figure 11.** One of the optimized structures of the H-bonded adduct of THF with syndio-hexa(4-vinylphenol) (B3LYP/6-31G(d)).

As we see, the preference of binding to a polymer (compared to a low-molecular-weight model) is about 2 kcal/mol in the case of pyridine. The reason for this is clearly seen in Figures 9 and 10, where the fully optimized structures of the PH-PVF adducts are reproduced. In both cases, weak CH···O bonds are clearly formed (in addition to the expected N···HO bond) in

the inner part of the PVF chain between one of the pyridine protons and the oxygen of the neighboring OH group. It is clear that such additional binding not only increases the equilibrium extent of pyridine bound to PVF but also slows substantially the frequency of rotation around the axis of the C−O−H−N bond. This fully explains the observed increase in the $R_{1B}^N$ value with increasing occupancy of PVF by pyridine.

As for binding of THF to PVF, no such weak CH−O bond could be found. The energy surface of the coordination space appears to have a lot of shallow minima so that the reproduced structure cannot be considered with assurance to correspond to a global minimum.

## Conclusions

Equilibrium hydrogen binding of two different acceptor ligands, namely, tetrahydrofuran (THF) and pyridine (PH), to a polymeric donor, namely, poly(4-vinylphenol) (PVF), was examined in this paper using NMR $^2$H quadrupolar and $^1$H longitudinal relaxation, PFG NMR self-diffusion measurement, and quantum mechanical calculations. The study was supplemented with a separate examination of hydrogen binding between a low-molecular-weight model of PVF, namely, 4-isopropylphenol, with pyridine.

The results are the following.

(1) All methods of investigation, namely, $^2$H NMR quadrupolar relaxation of the deuterons in the deutero analogues of the ligands tetrahydrofuran-$d_8$ (TDF) and pyridine-$d_5$ (PD), $^1$H longitudinal relaxation of their protonated forms, as well as $^1$H and $^2$H NMR PFG (namely, PGSE and PGSTE) measurement of their self-diffusion rate, can be used for establishing the extent of their binding to PVF or its model, providing that the data are renormalized to some standard viscosity using an added noninteracting compound ($CDCl_3$ or HMDSO) with a similar relaxation or self-diffusion rate. Under conditions of fast exchange, the molar fraction of the statistically bound ligand $\varphi$ is obtained from the general equation

$$\varphi = \frac{Q^N - Q_F^N}{Q_B^N - Q_F^N}$$

where $Q^N$ stands for $R_1^N$ (longitudinal quadrupolar $^2$H or dipolar $^1$H relaxation rate) or $D^N$ (self-diffusion coefficient) normalized to a standard viscosity regime and the subscripts B and F refer to the purely bound and free states, respectively.

The reliability of all the methods examined here was proven by the relative constancy of the equilibrium constants of binding calculated from the values of $\varphi$ obtained under a variety of ligand/PVF ratios under which a simple binding equilibrium can be expected.

(2) PD and PH bind somewhat stronger than TDF to PVF, although high-precision quantum-mechanical calculations do not predict such a large difference. Also, relaxation of PD exhibits slight anomalies at increasing PD/PVF ratio, which are not paralleled in self-diffusion experiments. Investigation of binding between a low-molecular-weight model of PVF, namely, 4-isopropylphenol, and PD does not show such anomalies.

(3) Using high-precision ab initio SCF-DFT calculations, it was shown that pyridine, in addition to a normal O−H···N bond, forms a weak C−H···O bond with the neighboring OH unit of PVF, which explains both the stronger overall bonding and the relaxation anomalies caused by a slowing of the rotation of pyridine around the axis of the O−H···N bond.

(4) As a marginal result, rotational diffusion around the axis of the (O−)H···N bond was found to be the main motion causing $^2$H or $^1$H relaxation in pyridine bound to PVF. In contrast to it, the axis of the main relaxation-causing rotation in the H-bonded adduct of pyridine with IPP (the low-molecular-weight model of PVF) appears to be approximately perpendicular to the former one.

**Acknowledgment.** The authors thank the Grant Agency of the Academy of Sciences of the Czech Republic for financial support given under the grant A4050206.

## References and Notes

(1) Lehn, J.-M. *Supramolecular Chemistry*; VCH Publishers: Weinheim, Germany, 1995.
(2) Tsuchida, E. *Macromolecular Complexes, Dynamic Interactions and Electronic Processes*; VCH Publishers: New York, 1991.
(3) Mich, J., Ed. *Modular Chemistry*; Proceedings, NATO ASI Series, Series C, Vol. 499; Kluwer Academic Publishers: Dordrecht, 1997.
(4) Weber, A., Ed. *Structure and Dynamics of Weakly Bound Molecular Complexes*; Kluwer Academic Publishers: Dordrecht, 1987.
(5) Kříž, J.; Kurková, D.; Dybal, J.; Oupick×c6, D. *J. Phys. Chem. A* **2000**, *104*, 10972.
(6) Kříž, J.; Dautzenberg, H. *J. Phys. Chem. A* **2001**, *105*, 3846.
(7) Kříž, J.; Dybal, J.; Dautzenberg, H. *J. Phys. Chem. A* **2001**, *105*, 7486.
(8) Kříž, J.; Dybal, J.; Kurková, D. *J. Phys. Chem. B* **2002**, *106*, 2175.
(9) Kříž, J.; Dybal, J.; Kurková, D. *J. Phys. Chem. A* **2002**, *106*, 7971−7981.
(10) Kříž, J.; Dautzenberg, H.; Dybal, J.; Kurková, D. *Langmuir* **2002**, *18*, 9594.
(11) Kříž, J.; Dybal, J.; Kurková, D. *J. Phys. Chem. B* **2003**, *107*, 12165.
(12) Pimentel, G. C.; McClellan, A. L. *The Hydrogen Bond*; W. H. Freeman and Co.: San Francisco, 1960.
(13) Desiraju, G. R.; Steiner, T. *The Weak Hydrogen Bond*; Oxford University Press: Oxford, 1999.
(14) Hubbard, P. S. *J. Chem. Phys.* **1969**, *51*, 1647.
(15) Hubbard, P. S. *J. Chem. Phys.* **1970**, *53*, 985.
(16) Bull, T. E. *J. Magn. Reson.* **1972**, *8*, 344.
(17) Stejskal, E. O.; Tanner, J. E. *J. Chem. Phys.* **1965**, *42*, 288.
(18) Tanner, J. E. *J. Chem. Phys.* **1970**, *52*, 2523.
(19) Dautzenberg, H. *Macromolecules* **1997**, *30*, 7810Z.
(20) Frisch, M. J.; Trucks, G. W.; Schlegel, H. B.; Scuseria, G. E.; Robb, M. A.; Cheeseman, J. R.; Zakrzewski, V. G.; Montgomery, J. A., Jr.; Stratmann, R. E.; Burant, J. C.; Dapprich, S.; Millam, J. M.; Daniels, A. D.; Kudin, K. N.; Strain, M. C.; Farkas, O.; Tomasi, J.; Barone, V.; Cossi, M.; Cammi, R.; Mennucci, B.; Pomelli, C.; Adamo, C.; Clifford, S.; Ochterski, J.; Petersson, G. A.; Ayala, P. Y.; Cui, Q.; Morokuma, K.; Malick, D. K.; Rabuck, A. D.; Raghavachari, K.; Foresman, J. B.; Cioslowski, J.; Ortiz, J. V.; Baboul, A. G.; Stefanov, B. B.; Liu, G.; Liashenko, A.; Piskorz, P.; Komaromi, I.; Gomperts, R.; Martin, R. L.; Fox, D. J.; Keith, T.; Al-Laham, M. A.; Peng, C. Y.; Nanayakkara, A.; Challacombe, M.; Gill, B.; Johnson, P. M. W.; Chen, W.; Wong, M. W.; Andres, J. L.; Gonzalez, C.; Head-Gordon, M.; Replogle, E. S.; Pople, J. A. *Gaussian 98*, Revision A.9; Gaussian, Inc.: Pittsburgh, PA, 1998.